High-frequency peaked radio sources

K. Iuzhanina[1] · A. Mikhailov[1] · Yu. Sotnikova[1] · V. Vlasyuk[1] · D. Kudryavtsev[1] · T. Mufakharov[1] · Yu.A. Kovalev[2] · Yu.Yu. Kovalev[3] · A. Popkov[2,4] · M. Kharinov[5] · M. Khabibullina[1] · A. Volvach[6] · L. Volvach[6]

[1] Special Astrophysical Observatory of the Russian Academy of Sciences, Nizhny Arkhyz, 369167 Russia
[2] Astro Space Center, Lebedev Physical Institute, Russian Academy of Sciences, Moscow, 117997 Russia
[3] Max-Planck-Institut für Radioastronomie, Auf dem Hügel 69, 53121 Bonn, Germany
[4] Moscow Institute of Physics and Technology, Institutsky per. 9, Dolgoprudny, 141700 Russia
[5] Institute of Applied Astronomy, Russian Academy of Sciences, Kutuzova Embankment 10, St. Petersburg, 191187 Russia
[6] Crimean Astrophysical Observatory of the Russian Academy of Sciences, Nauchny, 298409 Russia

DOI: 10.26119/2025-moc10 EDN: kaqgqa
eLocator: moc10

Abstract. We present a study of the multiwavelength properties of high-frequency peaked (HFP) radio sources. The study involved the simultaneous RATAN-600 measurements at frequencies of 1.2, 2.3, 4.7, 8.2, 11.2, and 22.3 GHz in 1997–2024, the RT-32 measurements at 5.05 and 8.63 GHz (IAA RAS), the RT-22 data at 36.8 GHz (CrAO RAS), and the literature data. It was found that the variability of the HFP synchrotron emission is relatively low, it reaches 0.02–0.23 on the monitoring time scale of 17–27 years. Modeling of the broadband radio spectra of HFP sources shows that they can be satisfactorily described both by synchrotron self-absorption and by free-free absorption. For two of the sources, PKS 1614+051 and PKS 2126−158, we calculated the evolution of the synchrotron self-absorption spectrum parameters and the magnetic field strength. The results of the optical spectroscopical study of PKS 1614+051 and PKS 2126−158, performed with the SCORPIO-1 spectrograph at the 6-meter telescope, revealed that they have different internal structures and are located in different galactic environments.

Keywords: galaxies: active; radio continuum: galaxies; methods: observational

1. Introduction

Understanding the origin and evolution of radio emission in extragalactic radio sources remains a central problem in modern astrophysics. In the evolutionary scenario, the physical size of a radio source is directly related to its age. Compact peaked-spectrum (PS) radio sources are therefore considered progenitors of classical radio galaxies (Fanti 1995). An empirical anticorrelation between the spectral peak frequency ν_m (also called the turnover frequency) and the projected linear size of the source (O'Dea & Baum 1997) indicates that high-frequency peaked (HFP) sources can be the youngest objects. HFP sources exhibit a convex broadband radio spectrum with a peak above 5 GHz and are thought to represent newly born radio sources with ages of only 10^2–10^3 years (Dallacasa et al. 2000; Dallacasa 2003). Their spectra are generally explained by synchrotron self-absorption (SSA) or free-free absorption (FFA) (see, e.g., Tingay & de Kool 2003).

The radio properties of HFP sources have been established mainly through bright-source samples (Dallacasa et al. 2000; Orienti et al. 2006). Two populations can be distinguished based on their spectral variability. One consists of the sources with a persistent convex spectrum and little variability, interpreted as genuinely young radio galaxies in an early evolutionary stage. The other consists of objects with strongly variable spectra, which are instead jet-dominated, beamed sources, i.e., blazars (Orienti et al. 2010). Supporting this view, Massaro et al. (2009) included all known PS sources in the Roma-BZCAT blazar catalogue. It is therefore important to distinguish between genuinely young HFP sources and blazar contaminants. Genuine HFP sources are compact symmetric objects or compact doubles, characterized by small projected sizes (≤ 100 pc), stable convex spectra, and weak variability. In contrast, blazar-like HFP sources are core-jet objects where a new, self-absorbed jet component can temporarily mimic a peaked spectrum at high frequencies. Their spectra evolve rapidly, showing variability and flattening over time. Thus, long-term spectral monitoring combined with the morphology obtained from very long baseline interferometry (VLBI) is essential to discriminate between young HFP galaxies/quasars and beamed blazar sources.

Multiwavelength studies of HFP sources are a powerful tool for investigating both the nature of young active galactic nuclei (AGNs) and the properties of their environment. Particularly intriguing are HFP sources at high redshifts ($z > 3$), corresponding to the cosmic epoch when the Universe was only about 15% of its present age, and AGNs were at the earliest evolutionary stages.

In this paper we analyze the long-term radio properties of five HFP candidates: J0927+3902, J0555+3948, J0428+3259, PKS 1614+051 (Sotnikova et al. 2024), and PKS 2126−158, selected from the RATAN-600 long-term blazar monitoring program, and investigate their variability and spectral evolution on time scales of up to nearly three decades.

2. Radio observations

The spectral flux densities were measured with the RATAN-600 radio telescope at 1.2, 2.3, 4.7, 8.2, 11.2, and 22.3 GHz in 1997–2024 (Kovalev et al. 1999; Mingaliev et al. 2012; Sotnikova et al. 2022), with the RT-22 radio telescope (CrAO RAS) at 36.8 GHz (PKS 1614+051, PKS 2126−158), and with the RT-32 radio telescope (IAA RAS) at 5.05 and 8.63 GHz. Since the observing frequencies of the RT-32 and RATAN-600 are close, we use their rounded values, 8 and 5 GHz, in the analysis. The other frequencies, 36.8, 22.3, 11.2, 2.3, and 1.2 GHz, are also used in rounded form: 37, 22, 11, 2, and 1 GHz. Some of the flux density measurements were taken from the interactive RATAN-600 Multi-Frequency Catalogue of Blazars—BLcat.[1] To construct quasi-simultaneous radio spectra, the spectral flux densities obtained with different telescopes must be averaged over a certain time period. We chose the interval of 39 days for PKS 1614+051 and PKS 2126−158 to get the maximum number of quasi-simultaneous radio spectra with flux densities measured at at least four frequencies. The quasi-simultaneous radio spectra of PKS 2126−158 are presented in Fig. 1.

[1] https://www.sao.ru/blcat/

Table 1. Timescale of observations

Name	z	Epoch	$N_{\rm sp}$
J0428+3259	0.47	2006–2023	13
J0555+3948	2.36	1997–2024	21
J0927+3902	0.69	1997–2023	16
PKS 1614+051	3.21	1997–2024	48
PKS 2126−158	3.26	1997–2024	65

Table 2. Fractional variability for HFP candidates at different frequencies

ν, GHz	PKS 1614+051	PKS 2126−158	J0927+3902	J0555+3948	J0428+3259
22	0.12±0.04	0.23±0.2	0.20±0.02	–	0.15±0.04
11	0.18±0.01	0.19±0.1	0.14±0.02	–	0.04±0.03
8	0.16±0.07	0.20±0.1	0.14±0.01	–	0.07±0.02
5	0.10±0.07	0.15±0.1	0.08±0.01	0.01±0.02	0.02±0.03

The redshifts z of the sources, the monitoring timescale, and the number of radio spectra $N_{\rm sp}$ that have been modeled are presented in Table 1. The longest timescales in the observer's frame of reference is 27 years (1997–2024), reached for the sources J0555+3948, PKS 1614+051, and PKS 2126−158. In the rest frame these timescales vary from 2 to 8 years.

3. Radio variability

The radio variability level is one of the HFP source classification criteria along with the frequency of the spectral maximum. It is generally considered that the variability of the HFP source radio emission does not exceed 0.2 (or 20%). We have evaluated the variability level using the fractional variability index $F_{\rm var}$ (Vaughan et al. 2003). The results at 5, 8, 11, and 22 GHz are presented in Table 2. The least variable sources are J0555+3948 and J0428+3259, with fractional variabilities at 5 GHz of 0.01 and 0.02 on monitoring timescales of 27 and 17 years, respectively. For J0555+3948 we could not calculate the fractional variability at 8, 11, and 22 GHz because the variance was less than the mean square error for these frequencies. J0927+3902 is more variable: $F_{\rm var} = 0.08$ at 5 GHz, 0.14 at 8 and 11 GHz, and 0.20 at 22 GHz. PKS 1614+051 and PKS 2126−158 are the most variable sources with fractional variability of 0.10 and 0.15 at 5 GHz and 0.18 and 0.19 at 11 GHz.

4. Modeling of broadband radio spectra

The broadband radio spectra have been modeled with the SSA model derived in (Türler 1999), homogeneous SSA model, homogeneous external FFA model, internal FFA model, and inhomogeneous external FFA model (see, e.g., Shao 2022). We compared how the models fit the observed data by calculating the Bayes factor (BF) from marginal likelihoods (evidence) using the UltraNest library (Buchner 2021). The model parameters in the case of SSA (Türler 1999) are as follows: turnover frequency ($\nu_{\rm m}$), flux density at the turnover frequency ($S_{\rm m}$), spectral index in the optically thin part of the spectrum ($\alpha_{\rm thin}$), and spectral index in the optically thick part of the spectrum ($\alpha_{\rm thick}$). In the case of inhomogeneous external FFA, the model parameters are the normalization parameter ($S_{\rm norm}$), turnover frequency (ν_p), spectral index (α), and gamma function parameter

(p) that corresponds to the distribution of absorbing clouds. Parameters for other models can be found in Shao (2022).

All of the aforementioned models described the majority of spectra of J0428+3259 with rather large errors. It can be assumed that in the case of J0428+3259 the double SSA + FFA model (see, Orienti & Dallacasa 2008 for details) should be used to fit the broadband radio spectra obtained with RATAN-600. The preferred double model reflects the contributions from multiple components, such as a compact SSA-dominated core along with an extended region absorbing via FFA. It means that the source has a hybrid nature: a compact synchrotron emission partially obscured by thermal plasma, which potentially indicates a young AGN embedded in a dense environment.

In the case of J0555+3948, the SSA (Türler 1999) and inhomogeneous FFA models provide the best fits in spectra modeling. The Bayes factor varies from 2 to 11 for different 1997–2022 spectra (moderate evidence in favor of SSA over inhomogeneous FFA). The SSA radio spectra modeled for the 1997–2024 period are presented in Fig. 2. In 1997 the ν_m value is 5.8 GHz, then in other epochs it increases and reaches 7.1 GHz. Since 2018 the turnover frequency has been no more than 5.1 GHz. The spectral flux density for this source has been decreasing for 23 years: in 1997 the flux density at the spectral peak was 6.4 Jy, in 2020 this value dropped to 4.2 Jy.

In modeling the J0927+3902 spectra, the SSA inhomogeneous FFA models are also best suited. The Bayes factors, when comparing these two models for the 2006–2010 spectra, range from 1 to 2, which is insignificant according to Jeffreys' scale and its modifications. For some spectra the model parameters have been obtained with large errors, which indicates that they should be fitted with a combination of different models or the lack of 1 GHz measurements at some epochs is the cause of the poor model approximation. Examples of modeled spectra for J0428+3259 and J0927+3902 are shown in Fig. 3.

For PKS 1614+051 the median Bayes factor is close to 1 (when comparing the SSA and inhomogeneous FFA models). For PKS 2126-158 it was noticed that some of the earlier spectra (1997–2012) have two peaks, which is illustrated in Fig. 4. The two-peak shape of the spectrum may indicate the appearance of a new component contributing to the high-frequency part of the spectrum. Perhaps such spectra should be modeled using, for example, the SSA + FFA model to allow for the contribution of the second component. For details on double models, see Shao (2022). The ν_m value for later epochs, where a two-peak structure has not been longer observed, does not show a decreasing trend. Despite the fact that PKS 2126−158 is the most variable source in the presented sample and has a core-jet morphology, its spectrum has remained convex for more than 27 years.

For PKS 1614+051 and PKS 2126−158, we have calculated magnetic field strength (for details see Sotnikova et al. 2024), and its value varies from 13 mG to 112 mG for PKS 1614+051 and from 4 mG to 90 mG for PKS 2126−158.

5. Optical spectroscopy

The spectroscopy of PKS 1614+051 and PKS 2126−158 was performed at the 6-meter telescope (BTA) with the SCORPIO-1 spectrograph (Afanasiev and Moiseev 2005) under good weather conditions: almost ideal atmosphere's clarity and a seeing of about 1.″5 (measured as the full width at half maximum of stellar spectra in individual exposures—this value is more correct for spectral data analysis). We used a 1.″2-wide slit in combination with the VPHG1200B grism from the SCORPIO-1 standard set.[2] The resulting spectral resolution was about 0.6 nm across the total spectral range between 360 and 540 nm. The total exposure was combined from several individual 10-min exposures. The details of the PKS 1614+051 observations, its optical spectrum, and the obtained results can be found in (Sotnikova et al. 2024).

[2] https://www.sao.ru/hq/lsfvo/devices/scorpio/scorpio.html

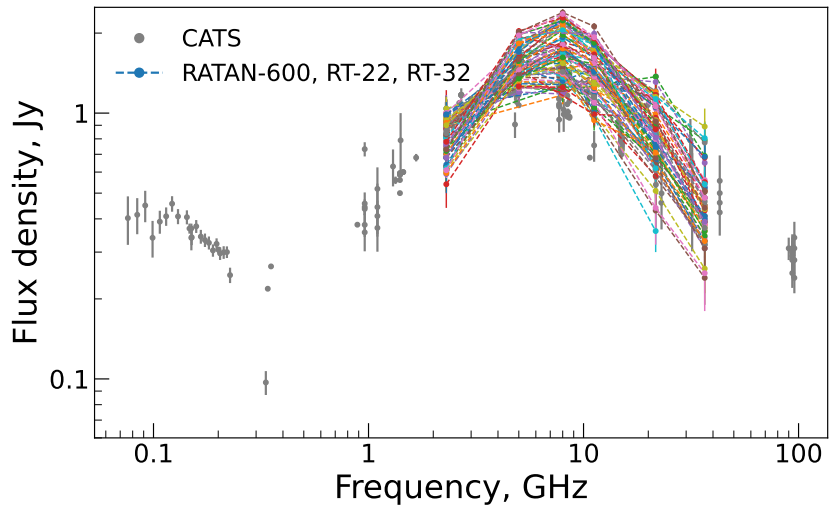

Figure 1. The quasi-simultaneous radio spectra of PKS 2126−158. The data from RATAN-600, RT-32, and RT-22 were obtained in 1997–2024 (colored). The measurements from the CATS database are shown with grey dots.

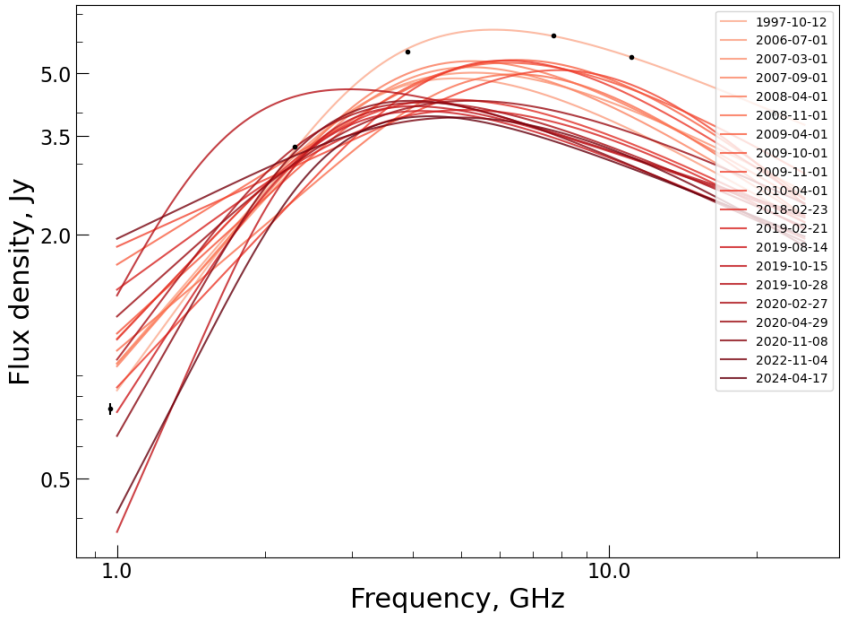

Figure 2. The SSA broadband radio spectra of J0555+3948 modeled for the period of 1997–2024. For illustration, the RATAN-600 data for the 1997-10-12 spectrum are shown with black dots.

In the observations of PKS 2126−158, the slit of the spectrograph was placed across the images of the blazar and the two nearest galaxies located to the west from it. The spectra are presented in Fig. 5. The spectrum of the blazar PKS 2126−158 shows a broad Lyα emission and a rich set of absorption lines in the spectral range between 380 and 520 nm. Most of them have been identified in the previous papers (e.g., Whiting et al. 2006). The obtained spectra of the galaxies have one significant emission line, which is identified with the forbidden line of ionized oxygen [OII] λ 372.7 nm. The redshifts of the foreground galaxies SDSS J212911.80-153841.2 and SDSS J212911.52−153840.8—numbers 1 and 2, respectively—are equal to 0.2392 ± 0.0003 and 0.2092 ± 0.0003. The PKS 2126−158 spectrum demonstrates the absorption doublets of [CaII] $\lambda\lambda$ 393.3 &

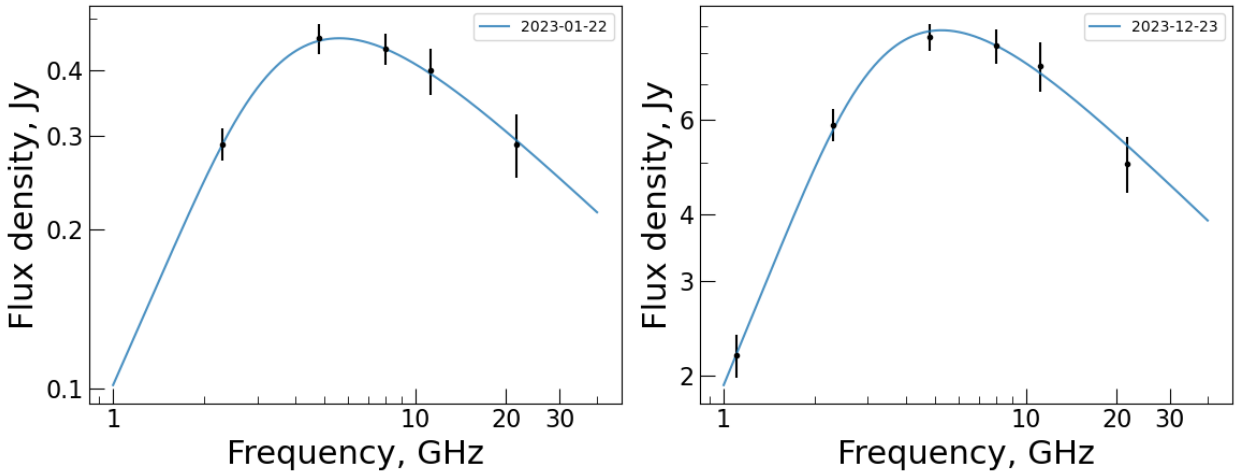

Figure 3. Examples of modeled spectra for J0428+3259 (left) and J0927+3902 (right). The RATAN-600 data are shown with black dots. The best fitting (SSA model) is shown with blue curves.

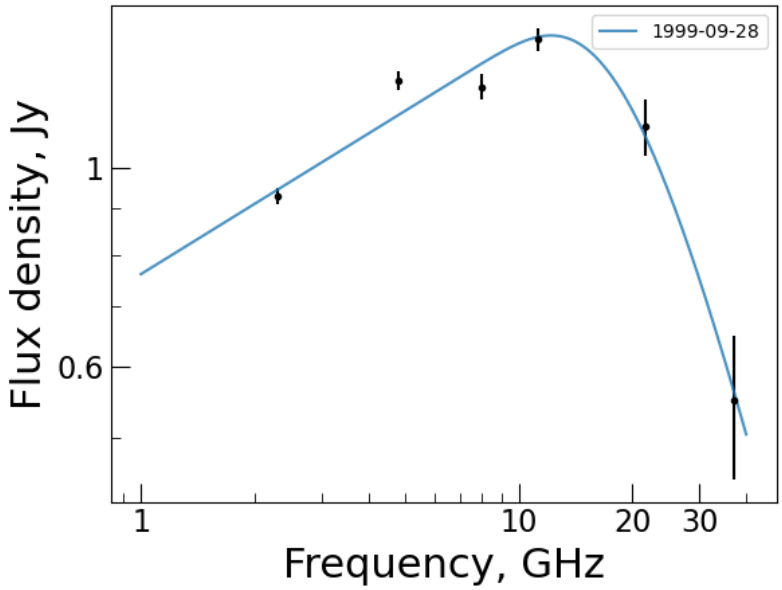

Figure 4. An example of the two-peaked spectrum for PKS 2126−158. The RATAN-600 data are shown with black dots. The best fitting (SSA model) is shown with a blue curve.

396.8 nm at the redshifts of these galaxies. The projected distances of the centers of the galaxies from the line of sight equal to 19 and 35 kpc, respectively.

The spectral studies of PKS 1614+051 and PKS 2126−158 conducted with BTA SCORPIO-1 and at other telescopes (Whiting et al. 2006; Husband et al. 2015) have shown significant differences both in their internal structure and in the presence/absence of a galactic environment. The blazar PKS 1614+051 is located in a dense galactic environment and shows the presence of a gaseous cloud (or disk) with size about 50 kpc; some nearby galaxies emit in Lyα (Husband et al. 2015). The blazar PKS 2126−158 is most likely isolated. Our data and the data taken with the Gemini Multi-Object Spectrograph (GMOS) show that all neighboring galaxies are located at intermediate distances: at redshifts between 0.2 and 0.8 (Whiting et al. 2006). More distant galaxies have not

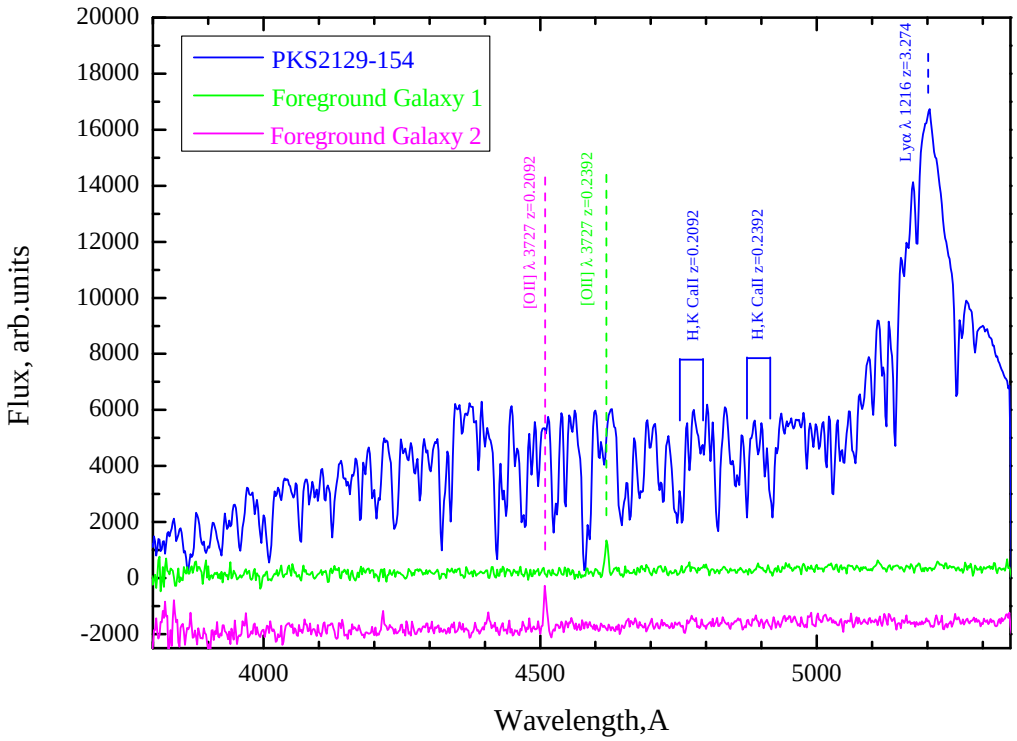

Figure 5. The optical spectra of PKS 2126−15 (blue line) and the neighboring galaxies numbered as 1 and 2 above. The data are presented in relative units. The spectra of galaxies are multiplied by a factor of 5 and shifted along the y-axis for better viewing. The vertical lines mark the emission lines of the blazar, the [OII] 372.7 nm emission lines in the galactic spectra, and the CaII absorptions.

yet been revealed in the field around the blazar. It was established that PS sources tend to reside in groups (Orienti et al. 2010).

6. Summary

We found that the radio variability of the considered HFP blazars is moderate on long timescales from 2 to 8 years (the rest frame). In general, fractional variability reaches ~ 0.2, which is less than the variability observed in most blazars. The flux densities of the HFP blazars have been changing smoothly for several decades, and their spectrum shapes remain almost constant, demonstrating insignificant shifts of the peak frequency.

There is no uniformity among the sources: while SSA is preferable in one case (J0555+3948), the choice between FFA and SSA cannot be made for J0927+3902 and PKS 1614+051 (BF ≤ 2), and a hybrid model is recommended for J0428+3259. These results support the idea that HFP sources are young compact AGNs, in many cases with SSA-driven turnovers determined by intrinsic jet properties (magnetic fields, particle densities). However, the FFA contribution (especially the external inhomogeneous FFA) implies interactions with the environment, such as absorption of the radio emission by ionized gas in the host galaxy.

The low radio variability level makes evolutionary trends more detectable than in the flaring sources. The anomaly in the behavior of the J0555+3948 flux density implies that not all HFP sources follow the standard models: additional processes such as adiabatic losses, entrainment, or variable accretion might be needed.

Despite their similar spectral shape and variability, PKS1614+051 and PKS2126−158 are located in different environments, as shown by a spectroscopic analysis. PKS 1614+051 is located in

a dense galactic environment with nearby galaxies emitting in Lyα and shows the presence of a gaseous cloud (or disk), while PKS 2126−158 is most likely isolated.

Acknowledgements Observations with the SAO RAS telescopes are supported by the Ministry of Science and Higher Education of the Russian Federation. The renovation of telescope equipment is currently provided within the national project "Science and Universities". This research has made use of the NASA/IPAC Extragalactic Database (NED), which is operated by the Jet Propulsion Laboratory, California Institute of Technology, under contract with the National Aeronautics and Space Administration; the CATS database, available on the Special Astrophysical Observatory website.

References

Afanasiev V.L. and Moiseev A.V., 2005, Astronomy Letters, 31, p. 194
Buchner J., 2021, Journal of Open Source Software, 6, 60
Dallacasa D., Stanghellini C., Centonza M., et al., 2000, Astronomy and Astrophysics, 363, p. 887
Dallacasa D., 2003, PASA, 20, 1, p. 79
Fanti C., Fanti R., Dallacasa D., et al., 1995, Astronomy and Astrophysics, 302, p. 317
Husband K., Bremer M.N., Stanway E.R., et al., 2015, Monthly Notices of the Royal Astronomical Society, 452, p. 2388
Kovalev Yu.Yu., Nizhelsky N., Kovalev Yu.A., et al., 1999, Astronomy and Astrophysics Supplement Series, 139, p. 545
Massaro E., Giommi P., Leto C., et al., 2009, Astronomy and Astrophysics, 495, 2, p. 691
Mingaliev M., Sotnikova Yu., Torniainen I., et al., 2012, Astronomy and Astrophysics, 544, id. A25
O'Dea C.P. and Baum S.A., 1997, Astronomical Journal, 113, p. 148
Orienti M. and Dallacasa D., 2008, Astronomy and Astrophysics, 487, p. 885
Orienti M., Dallacasa D., Stanghellini C., 2010, Monthly Notices of the Royal Astronomical Society, 408, 2, p. 1075
Orienti M., Dallacasa D., Tinti S., et al., 2006, Astronomy and Astrophysics, 450, 3, p. 959
Shao Yali, Wagg Jeff, Wang Ran, et al., 2022, Astronomy and Astrophysics, 659, id. A159
Sotnikova Yu., Mikhailov A., Volvach A., et al., 2024, Astrophysical Bulletin, 79, 4, p. 548
Sotnikova Yu., Mufakharov T., Mingaliev M., et al., 2022, Astrophysical Bulletin, 77, 4, p. 361
Tingay S.J. and de Kool M., 2003, Astronomical Journal, 126, 2, p. 723
Türler M., Courvoisier T.J.-L., and Paltani, S., 1999, Astronomy and Astrophysics, 349, p. 45
Vaughan S., Edelson R., Warwick R.S., et al., 2003, Monthly Notices of the Royal Astronomical Society, 345, 4, p. 1271
Whiting M.T., Webster R.L., Francis P.J., 2006, Monthly Notices of the Royal Astronomical Society, 368, p. 341